



# Human FAM173A is a mitochondrial lysine-specific methyltransferase that targets adenine nucleotide translocase and affects mitochondrial respiration

Received for publication, April 25, 2019, and in revised form, June 17, 2019. Published, Papers in Press, June 18, 2019, DOI 10.1074/jbc.RA119.009045

✉ Jędrzej M. Małecki<sup>‡1</sup>, Hanneke L. D. M. Willemsen<sup>§</sup>, Rita Pinto<sup>‡</sup>, Angela Y. Y. Ho<sup>‡</sup>, Anders Moen<sup>‡</sup>, Niels Eijkelkamp<sup>§</sup>, and ✉ Pål Ø. Falnes<sup>‡2</sup>

From the <sup>‡</sup>Department of Biosciences, Faculty of Mathematics and Natural Sciences, University of Oslo, 0316 Oslo, Norway and

<sup>§</sup>Laboratory of Translational Immunology (LTI), University Medical Center Utrecht, Utrecht University, 3584 EA Utrecht, The Netherlands

Edited by Ruma Banerjee

Lysine methylation is a common posttranslational modification of nuclear and cytoplasmic proteins but is also present in mitochondria. The human protein denoted “family with sequence similarity 173 member B” (FAM173B) was recently uncovered as a mitochondrial lysine (K)-specific methyltransferase (KMT) targeting the c-subunit of mitochondrial ATP synthase (ATPSc), and was therefore renamed ATPSc-KMT. We here set out to investigate the biochemical function of its yet uncharacterized paralogue FAM173A. We demonstrate that FAM173A localizes to mitochondria, mediated by a noncanonical targeting sequence that is partially retained in the mature protein. Immunoblotting analysis using methyllysine-specific antibodies revealed that FAM173A knock-out (KO) abrogates lysine methylation of a single mitochondrial protein in human cells. Mass spectrometry analysis identified this protein as adenine nucleotide translocase (ANT), represented by two highly similar isoforms ANT2 and ANT3. We found that methylation occurs at Lys-52 of ANT, which was previously reported to be trimethylated. Complementation of KO cells with WT or enzyme-dead FAM173A indicated that the enzymatic activity of FAM173A is required for ANT methylation at Lys-52 to occur. Both in human cells and in rat organs, Lys-52 was exclusively trimethylated, indicating that this modification is constitutive, rather than regulatory and dynamic. Moreover, FAM173A-deficient cells displayed increased mitochondrial respiration compared with FAM173A-proficient cells. In summary, we demonstrate that FAM173A is the long-sought KMT responsible for ANT methylation at Lys-52, and point out the functional significance of Lys-52 methylation in ANT. Based on the established naming nomenclature for KMTs, we propose to rename FAM173A to ANT-KMT (gene name *ANTKMT*).

Methylation is a common biochemical reaction that is catalyzed by specific methyltransferases (MTases)<sup>3</sup>, most of which use S-adenosylmethionine (AdoMet) as methyl donor (1). The human genome encodes more than 200 MTases, and for many of these enzymes the substrates still remain elusive, despite considerable recent progress (2). The majority of these enzymes belong to the so-called seven  $\beta$ -strand (7BS) class of MTases (1–3), and these methylate a variety of substrates, ranging from small metabolites to nucleic acids and proteins.

In proteins, several amino acid residues can be subject to methylation, including glutamine, histidine, arginine, and lysine (4–7). Lysine can become mono-, di-, or trimethylated, which increases the residue bulkiness and changes its hydrogen bonding capability but leaves the positive charge unaffected (8). Many of the human 7BS MTases have recently been identified as lysine (K)-specific MTases (KMTs) (9–24). Generally, these KMTs are highly specific, and seem to have evolved to target a particular lysine residue in a single protein or a group of closely related proteins (8).

Lysine methylation is a common modification of nuclear and cytosolic proteins, but is also present in mitochondria (25). Two soluble proteins residing in the mitochondrial matrix (the  $\beta$ -subunit of electron transfer flavoprotein (ETF $\beta$ ) and citrate synthase (CS)) contain methylated lysines, and recently the enzymes responsible for introducing these modifications were identified as mitochondrial 7BS KMTs. In particular, ETF $\beta$ -KMT (also known as METTL20) targets Lys-200 and Lys-203 in ETF $\beta$  (18, 22), whereas CS-KMT (also known as METTL12) methylates Lys-395 in CS (20, 23). Another prominent example of a lysine-methylated mitochondrial protein is the ATP synthase c-subunit (ATPSc), which resides in the inner mitochondrial membrane and is trimethylated at the matrix-exposed residue Lys-43 (26, 27). Very recently, we uncovered the previously uncharacterized protein denoted “family with

This work was supported by Research Council of Norway Grant FRIMEDBIO-240009 and Norwegian Cancer Society Grant 107744-PR-2007-0132 (to P. Ø. F.). This work was also supported by the Netherlands Organization for Scientific Research (NWO) Grant 016.VENI.192.053 (to H. L. D. M. W.). The authors declare that they have no conflicts of interest with the contents of this article.

This article contains Table S1 and Figs. S1 and S2.

<sup>1</sup> To whom correspondence may be addressed. E-mail: [j.m.malecki@ibv.uio.no](mailto:j.m.malecki@ibv.uio.no).

<sup>2</sup> To whom correspondence may be addressed. Tel.: 47-9115-1935; E-mail: [pal.falnes@ibv.uio.no](mailto:pal.falnes@ibv.uio.no).

<sup>3</sup> The abbreviations used are: MTase, methyltransferase; 7BS, seven  $\beta$ -strand; ANT, adenine nucleotide translocase; AntA, antimycin A; ATPSc, ATP synthase; ATPSc, ATPSc c-subunit; CS, citrate synthase; EGFP, enhanced green fluorescent protein; ETC, electron transport chain; ETF $\beta$ , electron transfer flavoprotein  $\beta$ -subunit; FCCP, carbonyl cyanide 4-(trifluoromethoxy)phenylhydrazone; KMT, lysine-specific methyltransferase; MTS, mitochondrial targeting sequence; OCR, oxygen consumption rate; preMT, pre-MTase sequence; TMD, transmembrane domain.

sequence similarity 173 member B" (FAM173B), as the mitochondrial KMT responsible for this methylation event, and the enzyme was therefore renamed ATPSc-KMT (21).

FAM173A is a paralogue of ATPSc-KMT that is present only in vertebrates. The two proteins share high degree of homology throughout their entire sequence, including the N-terminal region, which encompasses a predicted transmembrane domain (TMD) and a noncanonical mitochondrial targeting sequence (MTS) responsible for mitochondrial localization of ATPSc-KMT (21). Therefore, based on its strong sequence similarity to ATPSc-KMT, we suggested that also FAM173A is a mitochondrial 7BS-KMT that targets an inner mitochondrial membrane protein on a lysine residue that faces the matrix side (21).

The mitochondrial adenine nucleotide translocase (ANT) (also known as the adenine nucleotide translocator, ADP/ATP translocase, or ADP/ATP carrier), is a highly abundant transmembrane protein residing in the inner mitochondrial membrane, constituting up to 10% of total mitochondrial protein (28). The major function of ANT is to mediate the exchange of ADP in the intermembrane space, with ATP synthesized in the mitochondrial matrix, thus facilitating continuous synthesis of ATP by the mitochondrial ATP synthase complex (ATPS) (29, 30). Four paralogous genes (SLC25A4, -5, -6, and -31) encode for four different ANT isoforms in humans (ANT1, -2, -3, and -4, respectively), which share high degree of homology at the protein level (80–90% between various isoforms) but differ regarding their tissue-specific expression (29, 31). Interestingly, mammalian ANT1, -2, and -3 have been reported by several independent studies to be methylated at Lys-52 (32, 33) (numbering refers to the ANT precursor), but the responsible KMT has remained elusive.

In the present study we set out to identify the substrate(s) of human FAM173A. We found that FAM173A, similarly to ATPSc-KMT, was localized to mitochondria. Using FAM173A KO cells, we identified Lys-52 in ANT2 and ANT3 as targets of FAM173A. In addition, we found Lys-52 in ANT1 and ANT2 from rat to be present exclusively in the trimethylated form, indicating that this modification is constitutive *in vivo*. Finally, we observed that mitochondrial respiration was increased in FAM173A-deficient cells, thus pointing out the functional significance of Lys-52 methylation in ANT.

## Results

### Human FAM173A localizes to mitochondria

Human ATPSc-KMT (also known as FAM173B) is responsible for the methylation of Lys-43 in ATPSc (21), but the function of the paralogous protein, FAM173A, remains unknown. The sequence homology between FAM173A and ATPSc-KMT extends to their N-terminal regions, which contain a predicted TMD (21), followed by a stretch of conserved sequence (preMT) located immediately upstream of the MTase domain (Fig. 1A). The preMT sequence of ATPSc-KMT functions as a noncleavable MTS (21), thus suggesting that also FAM173A may be localized to mitochondria. To test this, we generated HeLa cells expressing a fusion protein where FAM173A was fused N-terminally to GFP (FAM173A-GFP), and its intracel-

lular localization was followed by fluorescence microscopy of live cells. We found that FAM173A-GFP was efficiently targeted to mitochondria, evidenced by its extensive colocalization with the dye MitoTracker Orange, which stains mitochondria (Fig. 1, B and C). A deletion mutant of FAM173A lacking the first 42 amino acids, including the TMD, was also efficiently targeted to mitochondria, whereas further deletion of the whole N-terminal region (the first 76 amino acids), including the TMD and the preMT sequence, completely abolished mitochondrial localization and resulted in homogenous staining of the entire cell (Fig. 1C). This suggests that the preMT sequence likely is responsible for the mitochondrial localization of FAM173A. Indeed, the isolated preMT sequence (amino acids 43–77 of FAM173A) was able to bring the GFP to mitochondria (Fig. 1, B and C).

Western blot analysis of mitoplast extracts from cells expressing FAM173A-FLAG (FLAG fused to the C terminus of FAM173A), revealed the presence of two species of FLAG-tagged protein (Fig. 1D) corresponding in size to the full-length FAM173A-FLAG protein (28.2 kDa), and a truncated version likely consisting of only the MTase domain (19.8 kDa; amino acids 78–235). In summary, microscopy and biochemical analyses demonstrate that FAM173A localizes to mitochondria, targeted by a noncanonical MTS, which together with the predicted TMD is partially retained in the mature protein.

### FAM173A is responsible for methylation of Lys-52 in mitochondrial adenine nucleotide translocase

To functionally characterize human FAM173A, the corresponding gene was disrupted in the haploid cell line HAP1, using CRISPR/Cas9 technology, with guide RNAs designed to target a sequence located upstream of motif "Post I," which contains a putatively catalytically important acidic residue (*i.e.* Glu-105 in FAM173A, see also Fig. 1A) required for catalytic activity of other 7BS KMTs (16, 20, 21). Through sequencing of genomic DNA, a clone of FAM173A KO cells was found that contained a 1-bp insertion in exon 3, resulting in generation of a truncated version of the FAM173A protein, which is devoid of motif Post I as well as the downstream portion of the MTase domain. The resulting protein is therefore predicted to be enzymatically inactive (for details, see "Experimental procedures").

Based on our recent findings on ATPSc-KMT, one may predict that also FAM173A is a KMT. To test this, we analyzed mitoplast extracts enriched in mitochondrial membranes for the presence of lysine-methylated proteins, using Western blotting and previously characterized anti-methyllysine antibodies (21, 23). Several lysine-methylated proteins were detected (Fig. 2, A and B), and, intriguingly, one band of an apparent mass of ~32 kDa was detected only in unmodified HAP1 (WT) cells, but not in FAM173A KO cells. To identify the protein(s) whose lysine methylation was abolished by FAM173A KO, mitochondrial membrane proteins were resolved by SDS-PAGE, and then the portion of the gel corresponding to the ~32 kDa band was digested with chymotrypsin, followed by MS analysis. Several mitochondrial proteins were identified in the analyzed material, including ANT2 and ANT3, which have been reported as trimethylated at Lys-52 (32, 33). In particular, two peptides with identical *m/z*, corre-

# Methylation of adenine nucleotide translocase by FAM173A

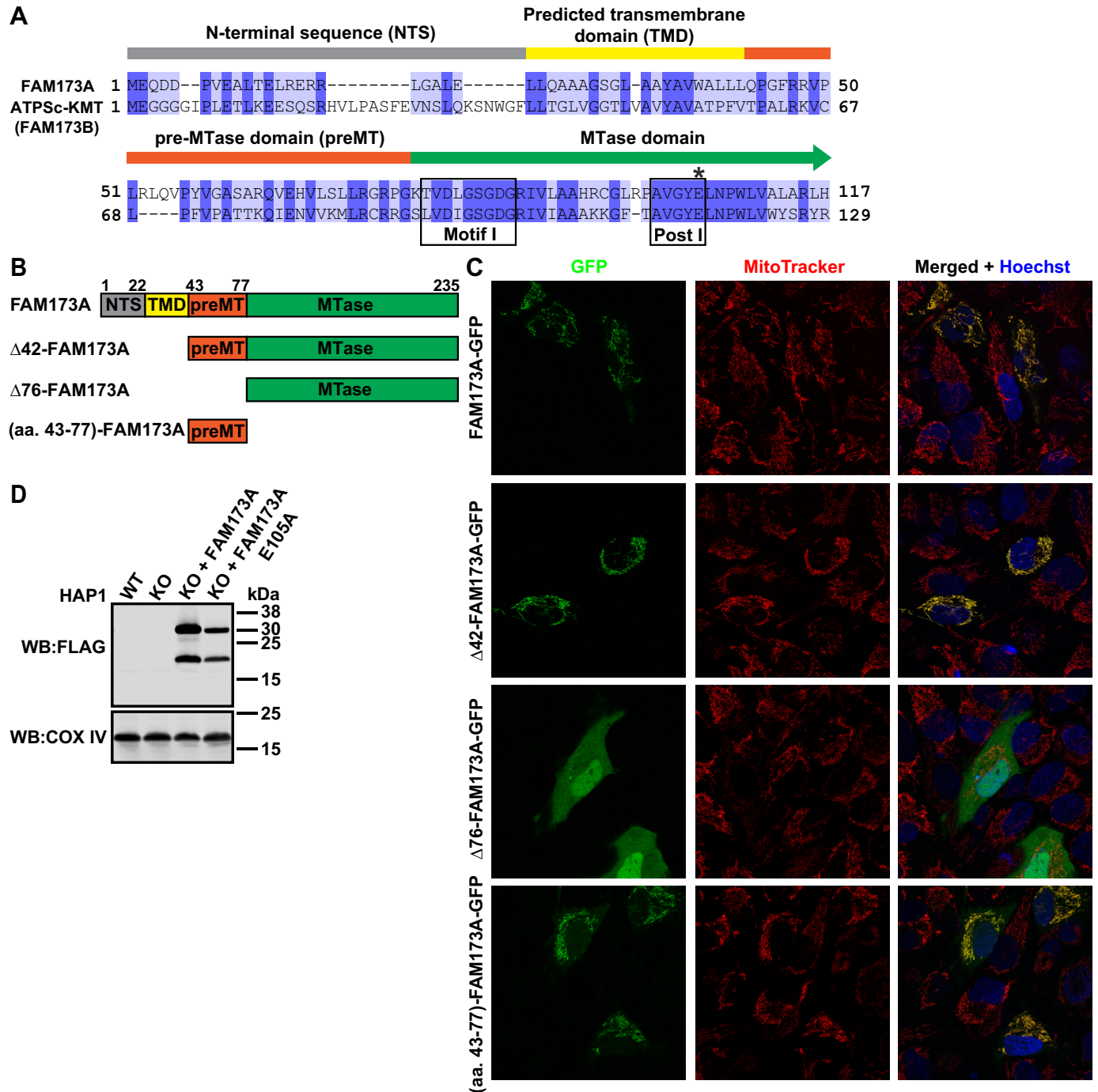


**Figure 1. A noncanonical MTS targets human FAM173A to mitochondria.** *A*, alignment of N-terminal parts of FAM173A and ATPSc-KMT (alias FAM173B) showing sequence elements present in their N-terminal region. Colors indicate the position of N-terminal sequence (NTS, gray), predicted TMD (yellow), preMT (orange), and the N-terminal portion of the MTase domain (green). Hallmark motifs of 7BS MTase domain are indicated by black boxes. The conserved acidic residue in motif Post I (Glu-105 in FAM173A), crucial for AdoMet binding, is marked with an asterisk. *B* and *C*, subcellular localization of FAM173A-derived GFP-fusion proteins. *B*, a schematic representation of the FAM173A-derived sequences used in *C*, with the various domains denoted as in *A*. *C*, confocal fluorescence microscopy images of live HeLa cells, stably transfected with plasmid encoding: FAM173A-GFP, (Δ42)-FAM173A-GFP, (Δ76)-FAM173A-GFP, or (amino acids 43–77)-FAM173A-GFP. Cells were counterstained with MitoTracker Orange to visualize mitochondria, and with Hoechst 33258 to visualize nuclei. Data were acquired through green (GFP), red (MitoTracker), and blue (Hoechst) channels and merged. *D*, Western blot analysis of proteins present in mitoplast extracts from HAP1 FAM173A KO cells complemented with FAM173A-FLAG, either WT or E105A-mutated, detected with anti-FLAG antibody. Expression of cytochrome c oxidase subunit IV (COX IV) is shown as a loading control.

sponding to residues 52–68 of human ANT2 and ANT3 were identified, appearing as a dual peak in the extracted ion chromatogram (Fig. 2C). MS/MS fragmentation analysis revealed that the major peak (with shorter retention time) represented the ANT2-derived peptide KGIIDCVVRIPKEQGVL (residues

52–68) (Fig. 2D), whereas the minor peak (with longer retention time) contained the highly similar ANT3-derived peptide KGIVDCIVRIPKEQGVL (Fig. 2E). Both peptides were almost exclusively found in the unmethylated state in FAM173A KO cells, but were predominantly (>95%) trimethylated in HAP1

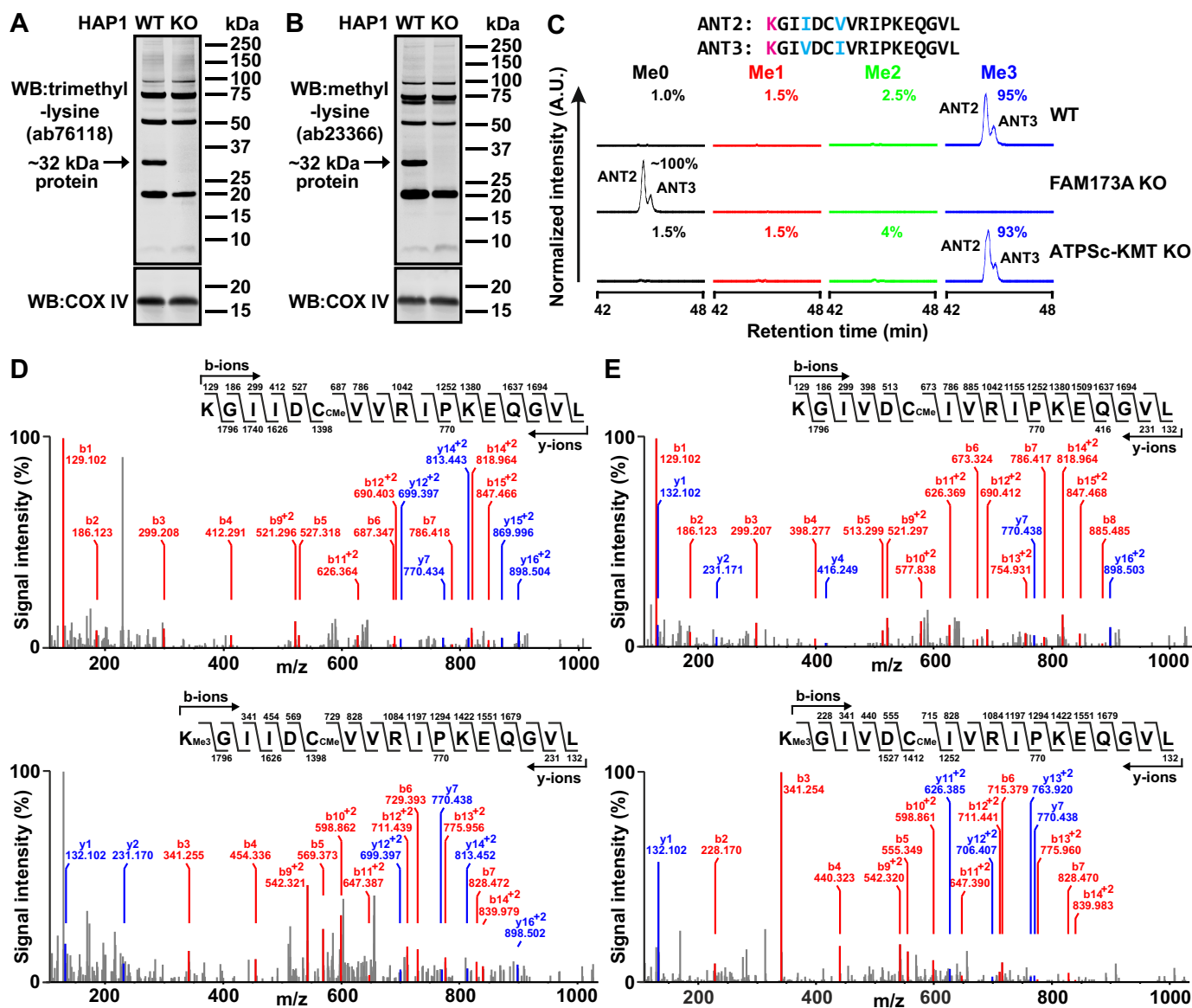


**Figure 2. Human FAM173A mediates methylation of Lys-52 in ANT inside cells.** *A* and *B*, Western blot analysis of methyllysine-containing proteins present in mitoplast extracts from HAP1 cells, either unmodified (WT) or FAM173A KO. Extracts enriched in mitochondrial membrane proteins were prepared from HAP1 WT or KO cells and resolved by SDS-PAGE. Proteins were transferred by Western blotting to a membrane, which was probed with antibodies against pan-trimethyllysine (*A*) or pan-methyllysine (*B*). In parallel, detection with anti-COX IV antibodies was performed (loading control). *C*, FAM173A KO abrogates ANT methylation in HAP1 cells. Extracts enriched in mitochondrial membrane proteins were prepared from HAP1 WT, FAM173A KO, and ATPSc-KMT KO cells, resolved by SDS-PAGE and the portion of the gel corresponding to the ~32 kDa region was chymotrypsin-digested and analyzed by MS. Shown are representative, normalized extracted ion chromatograms, gated for different methylation states of ANT-derived, chymotrypsin-generated peptides, encompassing residues 52–68 of human ANT2 and ANT3, present in indicated cells, with Lys-52 marked in *magenta*. Differences between ANT2 and ANT3 sequences are indicated in *cyan*. Percentages indicate the area under each peak, relative to the total area of all peaks. A.U., arbitrary units. *D*, MS/MS fragmentation spectra demonstrating absence of Lys-52 methylation in ANT2 from FAM173A KO cells (*top*) and presence of Lys-52 trimethylation in HAP1 WT cells (*bottom*). *E*, Same as in (*D*), but for ANT3. CMe, carbamidomethyl.

WT cells and in KO cells devoid of the paralogue ATPSc-KMT (Fig. 2C). MS/MS fragmentation analysis of these peptides revealed the methylation at Lys-52 (Fig. 2, *D* and *E*), *i.e.* the previously reported methylation site.

To confirm that FAM173A is directly responsible for methylation of ANT2 and ANT3 at Lys-52, we complemented FAM173A KO cells with an ectopically expressed gene encoding FAM173A-FLAG or a corresponding E105A-mutated FAM173A-FLAG, predicted to be enzymatically inactive (Fig. 1D). We then assessed the methylation status of ANT2 and ANT3 in the complemented cells. We observed that comple-

mentation with FAM173A largely restored trimethylation of Lys-52 to levels similar to those observed in WT cells, whereas complementation with E105A-mutated FAM173A failed to restore methylation (Fig. 3). These results firmly demonstrate that the enzymatic activity of FAM173A is necessary for Lys-52 methylation of ANT2 and ANT3 in cells.

#### ANT from rat is constitutively trimethylated at Lys-52

To investigate the methylation status of Lys-52 in ANT *in vivo*, we analyzed a panel of rat organs. Similarly to previous reports (31), we found that expression of the various ANT iso-

## Methylation of adenine nucleotide translocase by FAM173A

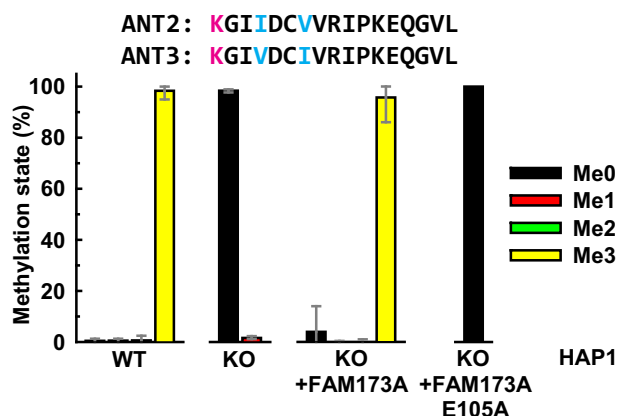


**Figure 3. Complementation of FAM173A KO cells with FAM173A restores the methylation of Lys-52 in ANT.** Extracts enriched in mitochondrial membrane proteins were prepared from HAP1 WT, FAM173A KO, or KO cells expressing FLAG-tagged FAM173A, either nonmutated or E105A-mutated (expression of FLAG-tagged proteins was verified in Fig. 1D), and analyzed by MS as in Fig. 2. Shown are the mean relative intensities of MS signals, gated for different methylation states of the indicated, ANT-derived peptides, encompassing residues 52–68 of human ANT2 and ANT3, with Lys-52 marked in magenta. Differences between ANT2 and ANT3 sequences are indicated in cyan. Error bars indicate the range of values from three independent analyses of each cell line.

forms varied greatly between the investigated organs (Fig. 4A). Although ANT1 was expressed mainly in rat muscle, heart, and brain, the ANT2 isoform was expressed mostly in liver, kidney, lung, and brain. (Note: expression of ANT3 was not detected in any of the tested organs). Importantly, both ANT1 and ANT2 were in all cases found to be fully trimethylated at Lys-52 (Fig. 4, B and C), indicating that this modification is constitutive *in vivo*.

### Lack of FAM173A activity increases mitochondrial respiration

ANT mediates the exchange of ADP for ATP across the inner mitochondrial membrane, and its translocase activity may influence the rate of ATP synthesis by the ATPS. Because mitochondrial ATP synthesis is driven by the respiratory chain, which consumes molecular oxygen, we tested whether FAM173A-mediated methylation of ANT at Lys-52 influenced mitochondrial respiration. To this end, we used a Seahorse analyzer to measure the oxygen consumption rate (OCR) in mitochondria isolated from HAP1-derived FAM173A-proficient cells (*i.e.* WT and FAM173A KO cells complemented with FAM173A) or FAM173A-deficient cells (*i.e.* FAM173A KO, and KO cells complemented with E105A-mutated FAM173A). Isolated mitochondria were incubated with succinate as source of electrons for Complex II of the electron transport chain (ETC) and rotenone (inhibitor of Complex I), and OCR was measured under basal conditions ( $OCR_{\text{basal}}$ ) and after sequential addition of a) ADP ( $OCR_{\text{ADP}}$ ), b) oligomycin (inhibitor of ATP synthesis by ATPS;  $OCR_{\text{oligomycin}}$ ), c) FCCP (uncoupling protonophore that dissipates mitochondrial membrane potential;  $OCR_{\text{FCCP}}$ ), and d) antimycin A (inhibitor of Complex III of ETC;  $OCR_{\text{AntA}}$ ). This allows assessment of the various states of mitochondrial respiration, *i.e.* State II, basal respiration ( $OCR_{\text{basal}} - OCR_{\text{AntA}}$ ); State III, respiration stimulated by ATP synthesis from ADP and phosphate ( $OCR_{\text{ADP}} - OCR_{\text{AntA}}$ ); State IV<sub>o</sub>, respiration because of proton leak in the presence of

oligomycin ( $OCR_{\text{oligomycin}} - OCR_{\text{AntA}}$ ); and State III<sub>u</sub>, respiration in presence of mitochondrial uncoupling agent ( $OCR_{\text{FCCP}} - OCR_{\text{AntA}}$ ). We found that in FAM173A-deficient cells, State II and State III respiration were both increased by ~50% compared with the FAM173A-proficient cells (Fig. 5A). Similarly, respiration in the presence of oligomycin or the uncoupling agent FCCP, were also increased in FAM173A-deficient cells. Reassuringly, in all cell lines tested, the level of various mitochondrial proteins was similar, including cytochrome *c* oxidase subunit IV (COX IV) (a component of ETC), ATPSc and ATP5A (the subunits of ATPS complex), as well as ANT2 (Fig. 5B). In summary, these results show that lack of active FAM173A results in a strong increase of mitochondrial respiration.

### Discussion

In this study, we have unraveled the biochemical function of a novel human MTase, FAM173A, which is present only in vertebrates and is a paralogue of ATPSc-KMT, which is ubiquitously found in all metazoans. We demonstrated that FAM173A is the long-sought KMT responsible for methylation of Lys-52 in the mitochondrial ANT. Moreover, we detected only trimethylated Lys-52 in ANT from rat, indicating that this modification is constitutive *in vivo*. Finally, we found that lack of FAM173A activity results in strongly increased mitochondrial respiration.

We showed that FAM173A localizes to mitochondria, and that its preMT sequence is responsible for this subcellular localization (Fig. 1C). Additionally, Western blotting of mitoplast extracts enriched in mitochondrial membranes detected the full-length form of FAM173A (Fig. 1D), suggesting that the predicted TMD anchors the enzyme to the membrane. Furthermore, the target of FAM173A, ANT, is membrane-embedded, and contains six transmembrane  $\alpha$ -helical regions that transverse the inner mitochondrial membrane forming a pore, through which ADP and ATP are being exchanged (34) (Fig. 6). Lys-52 is part of a large solvent-exposed segment that connects the first and the second transmembrane  $\alpha$ -helix of the pore and faces the mitochondrial matrix. Thus, we favor a model where intact FAM173A is inserted into the inner mitochondrial membrane *via* its TMD, and its MTase domain faces the matrix and makes direct contacts with its membrane-embedded substrate, ANT (Fig. 6). Recently, we proposed a similar model for subcellular localization of ATPSc-KMT, which targets Lys-43 in ATPSc (21) (Fig. 6).

In all *Metazoa*, ATPSc forms a porelike structure composed of eight subunits, the so-called  $c_8$ -ring, which is localized in the mitochondrial inner membrane. Lys-43 is part of a solvent-exposed loop connecting the two transmembrane  $\alpha$ -helices and faces the matrix. Molecular dynamics simulations implicated Lys-43 of ATPSc in binding of cardiolipin (35), an abundant anionic lipid in the inner mitochondrial membrane. Interestingly, ANT also binds cardiolipin, and one of the three cardiolipin molecules found in ANT crystal structures is located in the vicinity of Lys-52 (Fig. 6) (34, 36). In fact, Lys-52 is part of one of three conserved [Y/F]XG motifs present in ANT (where X denotes any amino acid, *e.g.* Lys-52) that are located in the matrix-exposed segments connecting the odd-

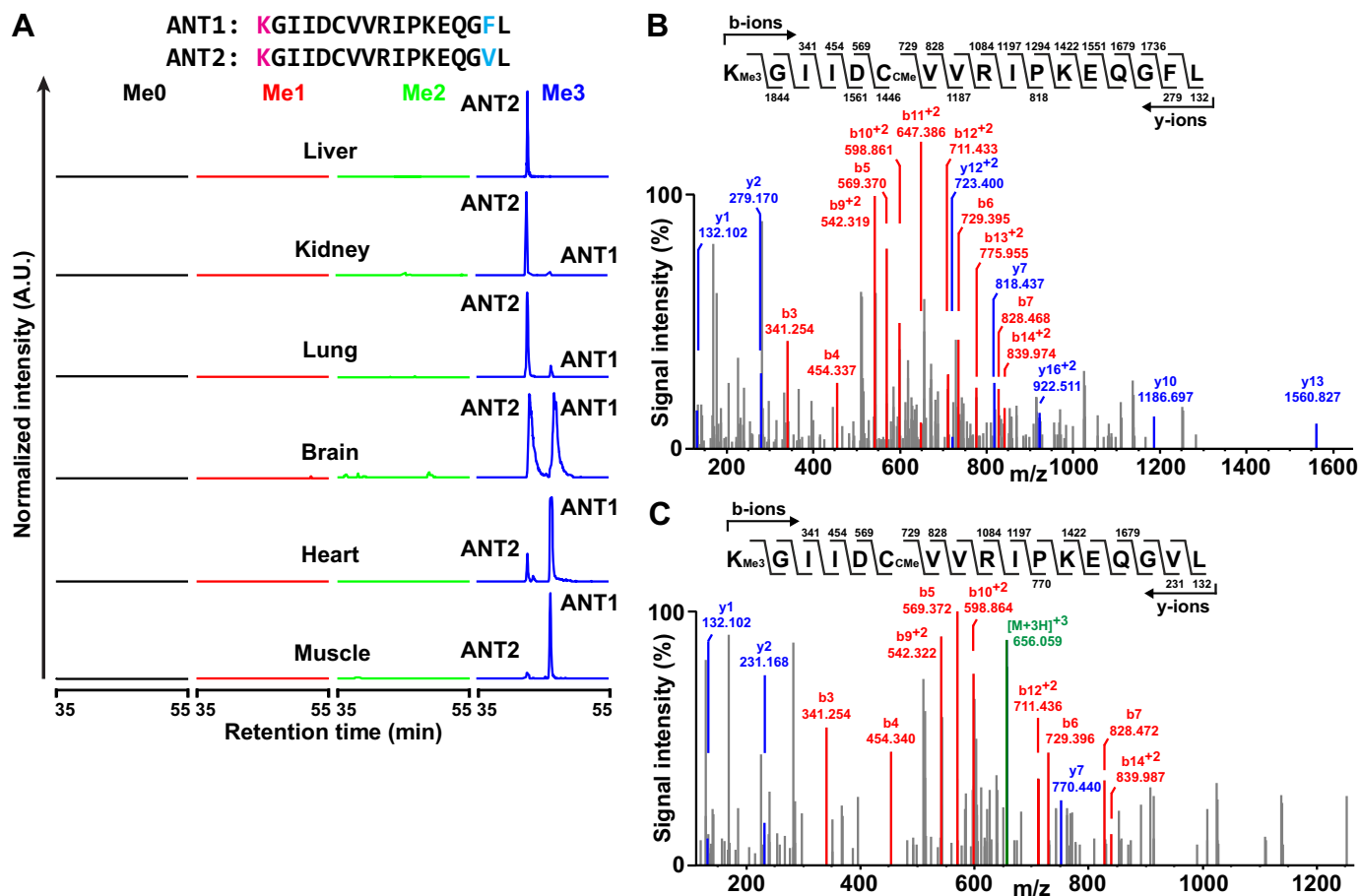


**Figure 4.** ANT1 and ANT2 from rat are fully trimethylated at Lys-52. *A*, Extracts enriched in mitochondrial membrane proteins were prepared from indicated rat organs, resolved by SDS-PAGE and a portion of gel corresponding to ANT was chymotrypsin-digested and analyzed by MS. Shown are representative, normalized extracted ion chromatograms, gated for different methylation states of ANT-derived, chymotrypsin-generated peptides, encompassing residues 52–68 of ANT1 and ANT2 present in indicated organs. MS signals and amino acid sequences corresponding to ANT1 and ANT2-derived peptides are indicated, with Lys-52 marked in *magenta*. Differences between ANT1 and ANT2 sequences are indicated in *cyan*. *B*, MS/MS fragmentation spectra demonstrating trimethylation of Lys-52 in ANT1 from rat heart. *C*, MS/MS fragmentation spectra demonstrating trimethylation of Lys-52 in ANT2 from rat kidney. CMe, carbamidomethyl.

and even-numbered transmembrane helices, which allow binding of three cardiolipin molecules (34, 37). Interactions of ANT with cardiolipin are important for self-association of ANT, and influence its oligomerization (36, 38). Thus, both FAM173A and ATPSc-KMT target a pore-forming protein that is embedded in the inner mitochondrial membrane, and the targeted lysine residue is involved in cardiolipin binding. Consequently, one may speculate that, for both ATPSc and ANT, lysine methylation influences the binding of cardiolipin, although theoretical simulations yet have failed to show strong effects in this respect (35, 37).

In HAP1-derived cells, the absence of FAM173A activity, *i.e.* lack of methylated Lys-52 in ANT, was accompanied by increased State II and State III mitochondrial respiration (Fig. 5A), which are both linked to ATP synthesis. Hence, one potential explanation is that methylation of ANT reduces its translocase activity, and the limited ADP/ATP exchange across the mitochondrial inner membrane leads to decreased ATP synthesis and decreased respiration in FAM173A-proficient mitochondria.

Apart from its classical function in ADP/ATP exchange, ANT has been implicated in the formation of mitochondrial

transition pore and apoptotic cell death (reviewed in Ref. 29). ANT2 was also reported as part of the mitotic spindle-associated MMXD complex, and may play a role in chromosome segregation (39). Our data show that State IV<sub>o</sub> and State III<sub>u</sub> respiration, which are unrelated to ATP synthesis, were also increased in FAM173A-deficient cells (Fig. 5A), suggesting that ANT methylation may reduce the permeability of the inner mitochondrial membrane to proton leak and/or reduce the performance of the ETC. The latter is a valid possibility, because ANT was reported to interact with respiratory subcomplexes in a cardiolipin-dependent fashion (38, 40). How canonical and noncanonical ANT functions, as well as the ANT interactome, are affected by Lys-52 methylation will likely be the subject of future studies.

Under standard laboratory conditions, Lys-52 of ANT was found exclusively in the trimethylated state both in human cell lines and in organs from adult rats. This suggested that ANT methylation is constitutive, rather than dynamic. However, it cannot be excluded that under some (yet to be identified) stress conditions, or during certain developmental stages, ANT methylation is more dynamic and plays a role in regulating metabolism.

## Methylation of adenine nucleotide translocase by FAM173A

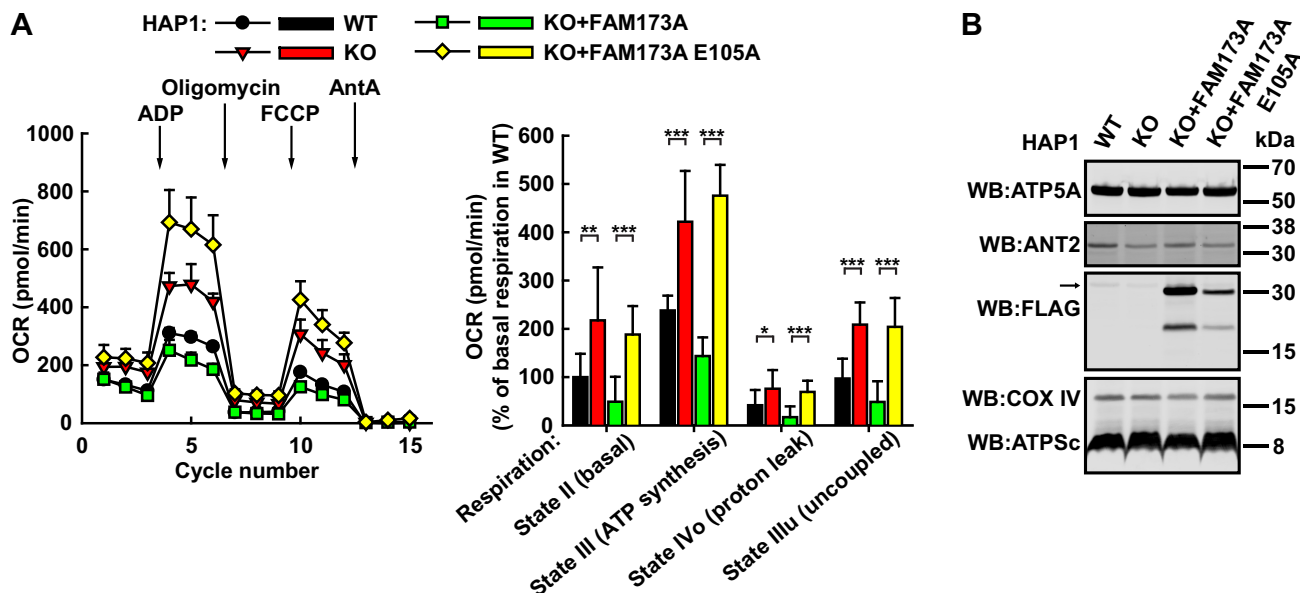


**Figure 5. Lack of active FAM173A increases mitochondrial respiration in HAP1-derived cells.** *A*, mitochondrial respiration is increased in FAM173A-deficient cells. Mitochondria were isolated from unmodified HAP1 (WT), FAM173A KO, or KO cells complemented with FLAG-tagged FAM173A, either non-mutated or E105A-mutated. OCRs of isolated mitochondria (15  $\mu$ g of mitochondrial protein) were measured by Seahorse analyzer, in the presence of succinate and rotenone, under basal conditions, and after sequential addition of ADP, oligomycin, FCCP, and AntA. *Left*, typical OCR traces from a representative experiment, with *arrows* indicating the time of addition of the indicated compounds. *Error bars* represent the S.D. ( $n = 5$ ). *Right*, mitochondrial respiration dissected into individual states, *i.e.* State II (basal respiration), State III (respiration after addition of ADP, because of ATP synthesis), State IVo (respiration in presence of oligomycin, because of proton leak), and State IIIu (respiration in presence of mitochondrial uncoupler FCCP). Shown are the average values from two independent experiments. *Error bars* represent the S.D. ( $n = 10$ ). \*,  $p$  value  $< 0.1$ ; \*\*,  $p$  value  $< 0.01$ ; \*\*\*,  $p$  value  $< 0.001$ . *B*, Western blot analysis of mitoplast extracts from HAP1-derived cells. Extracts enriched in mitochondrial membrane proteins were prepared from cells indicated as in (*A*). 40  $\mu$ g of protein from extracts were resolved by SDS-PAGE and transferred by Western blotting (WB) to a membrane, which was probed with anti-ANT2 antibody. The membrane was then sequentially reprobed with anti-ATPSc, anti-COX IV, anti-FLAG, and anti-ATP5A antibodies. *Arrow* indicates the position of ANT2 band visible on the membrane probed with anti-FLAG antibody, which results from the previous probing of this membrane with anti-ANT2 antibody. Shown are images from a representative experiment.

In recent years, we have unraveled the biochemical function of several human 7BS KMTs, and in the majority of these cases we could demonstrate a robust *in vitro* enzymatic activity of the recombinant KMT on the relevant substrate in cell extracts (typically from KMT KO cells) (13–15, 18–20, 41). Despite numerous efforts we were, however, unable to demonstrate KMT activity of recombinant FAM173A on ANT from mitoplasts from FAM173A KO cells. This may have several alternative explanations. For example, methylation may only occur when the substrate protein is found in a certain folding state or structural context, or specific co-factors are required. Indeed, we previously found that valosine containing protein (VCP)-KMT-mediated methylation of Lys-315 occurs only on monomeric VCP, prior to its assembly into hexamer (16), and that the eEF1A-KMT3-mediated methylation of Lys-165 in eEF1A is strictly dependent on ATP and tRNA (19). ANT is an oligomeric transmembrane protein that associates with other proteins to form supramolecular complexes (38), and these interactions could affect the accessibility of Lys-52. However, our observation that enzymatically active FAM173A is required for ANT methylation in cells, taken together with FAM173A being a putative KMT, strongly indicates that this MTase directly catalyzes methylation of ANT at Lys-52.

ANT proteins are part of a larger family of mitochondrial transporters, namely the SLC25 family, and several other members contain a Lys residue at the position corresponding to Lys-52 in ANT (Fig. S1A). Because of high sequence homology with ANT, one may speculate that FAM173A also targets other

SLC25 family members. However, none of the other SLC25 members have been reported to contain a methylated lysine residue at the relevant position, except for Aralar1, which was observed as monomethylated at Lys-370 in a single report (25). We were unable to verify the methylation status of Aralar1 at Lys-370, but we found Lys-101 (corresponding to Lys-52 in ANT) in the rat and human mitochondrial phosphate carrier to be completely unmethylated (Fig. S1, B–D). Thus, there are so far no convincing indications that proteins other than ANT are targeted by FAM173A.

Although all vertebrates contain genes encoding the paralogous FAM173A and ATPSc-KMT proteins, invertebrate animals have only one gene that codes for a single FAM173-like protein. Previously, we showed that the FAM173-like protein from nematode *Caenorhabditis elegans*, Y39A1A.21, trimethylated Lys-43 in ATPSc, similarly to human ATPSc-KMT (21). Thus, one may speculate that Y39A1A.21 also targets ANT, but this does not appear to be the case, because we found *C. elegans* ANT to be unmethylated at Lys-56, the residue corresponding to Lys-52 in human ANT (Fig. S2). Consequently, we favor the scenario that ATPSc-KMT represents the primordial enzyme from which the vertebrate-specific FAM173A evolved after a gene duplication event.

In recent years, several novel human 7BS KMTs that target a single protein have been discovered, and a naming nomenclature based on their substrate specificity has been established. In particular, FAM173B was recently renamed ATPSc-KMT (gene name *ATPSCKMT*) (21), and, accordingly, we here pro-

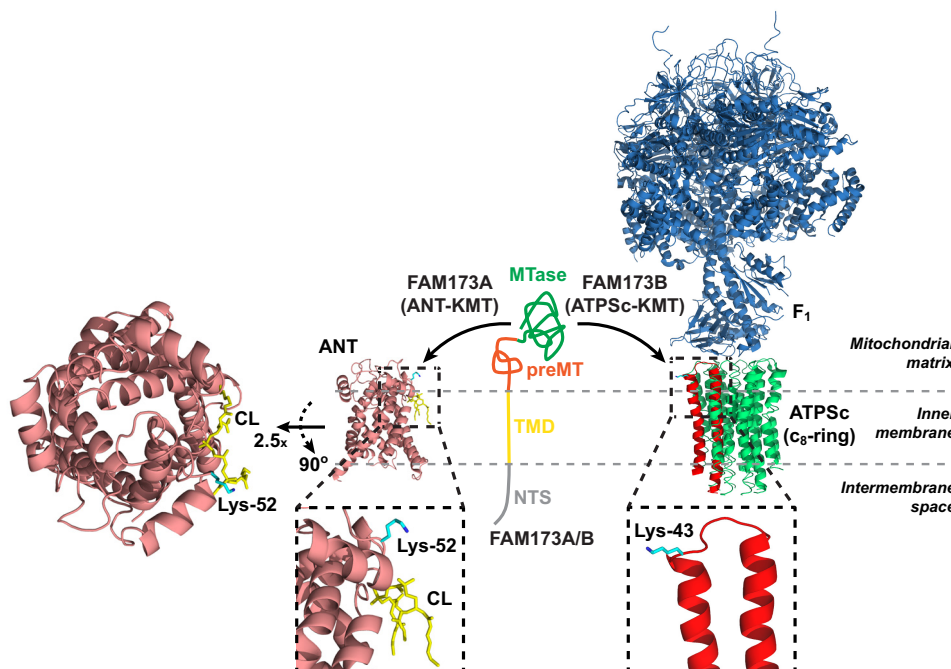


**Figure 6. The paralogous KMTs, FAM173A/ANT-KMT, and FAM173B/ATPSc-KMT, target similarly positioned lysines in ANT and ATPSc.** *Left*, structural representation of bovine ANT, and its topology in the inner mitochondrial membrane, generated from a previously published structure (34) (PDB ID: 1OKC). Rotation and magnification (2.5 $\times$ ) of ANT was performed to better visualize the pore-forming structure of ANT, and the positions of Lys-52 (cyan) and cardiolipin (CL; yellow). A model for the submitochondrial localization of FAM173A/B is presented in the center, with annotations and coloring as in Fig. 1. *Right*, structural representation of F<sub>1</sub>-c<sub>8</sub> subcomplex of bovine ATP synthase, and its topology in the inner mitochondrial membrane, generated from a previously published structure (45) (PDB ID: 2XND) and further adapted from Malecki *et al.* (21). The F<sub>1</sub> subcomplex is shown in blue, and ATPSc are shown in green, except for one of the eight protomers of the c<sub>8</sub>-ring, which is shown in red, and Lys-43 is here indicated in cyan.

pose to rename FAM173A to ANT-KMT (gene name *ANTKMT*).

## Experimental procedures

### Gene cloning and mutagenesis

The plasmid constructs and the strategy to generate them are described in detail in Table S1. In brief, open reading frames were amplified by PCR, and cloned into indicated vectors by standard ligation-dependent cloning, or by ligation-independent cloning using In-Fusion<sup>®</sup> HD Cloning Plus kit (Takara). Mutations within open reading frames were introduced by site-directed mutagenesis using PCR splicing by overhang extension (PCR SOEing) as described previously (21). Sanger sequencing was used to verify all cloned constructs.

### Bioinformatics analysis

Sequence alignments were generated using algorithms embedded in the JalView interface (<http://www.jalview.org/>) (42).<sup>4</sup>

### Cell cultures

HeLa cells were grown in RPMI 1640 GlutaMAX medium supplemented with 10% (v/v) FBS and 100 units/ml of penicillin and 0.1 mg/ml streptomycin. HAP1-derived cells were grown in Iscove's modified Dulbecco's medium GlutaMAX medium supplemented with 10% FBS and 100 units/ml of penicillin and 0.1 mg/ml streptomycin.

### Generation of HAP1-derived stable cell lines

HAP1 FAM173A KO cells were generated as a custom (non-exclusive) project by Horizon Genomics (Vienna, Austria). The *FAM173A* gene was disrupted in haploid HAP1 parental cells using CRISPR-Cas9, with guide RNA designed to target part of exon located upstream of motif Post I, which is required for enzymatic activity of 7BS MTases. Individual clones were selected by limiting dilution, and frame-shifting events within the targeted gene were determined by sequencing of genomic DNA. The FAM173A-deficient cell line used in this study contains a 1-bp insertion within exon 3, resulting in generation of a truncated version of the FAM173A protein devoid of motif Post I, consisting of the initial 101 amino acids of FAM173A, followed by 50 residues of out-of-frame sequence, and this cell line is commercially available (Horizon Discovery, HZGHC000532c005). Complementation of FAM173A KO cells was performed similarly as described previously (20) by transfection with a p3xFLAG-CMV-14-derived plasmid encoding either WT or E105A-mutated human FAM173A, all bearing a C-terminal 3xFLAG-tag. Transfected cells were selected with 1 mg/ml geneticin (Gibco) and expanded in medium containing geneticin. Individual clones of complemented cells were screened by Western blotting for the presence of FLAG-tag and COX IV (as loading control), using appropriate antibodies (see "Western blot analysis"). Generation of HAP1 ATPSc-KMT (FAM173B) KO cells has been described in detail in Ref. 21, and this cell line is also commercially available (Horizon Discovery, HZGHC000533c006).

<sup>4</sup> Please note that the JBC is not responsible for the long-term archiving and maintenance of this site or any other third party hosted site.



## Methylation of adenine nucleotide translocase by FAM173A

### Generation of stably transfected HeLa cells and fluorescence microscopy

HeLa cells were stably transfected with pEGFP-N1-derived plasmids (Clontech), encoding human full-length FAM173A, its variants with initial 42 or 76 amino acids deleted ( $\Delta 42$  or  $\Delta 76$ ), or a fragment consisting only of amino acids 43–77 of FAM173A, all fused to the N terminus of enhanced GFP (EGFP). 24 h after transfection, cells were selected with 1 mg/ml geneticin (Gibco) and the surviving cells were expanded in medium containing geneticin. Pooled surviving cells were seeded in 35-mm dishes with glass bottom (MatTek) and grown until ~50% confluence. Living cells were stained with 50 nM MitoTracker Orange CMTMRos (Molecular Probes) and 0.5  $\mu$ g/ml Hoechst 33258 (Sigma) to visualize the mitochondria and the nuclei, respectively. Cells were imaged using an Olympus FluoView 1000 (IX81) inverted confocal fluorescence microscopy system, equipped with a PlanApo N 60 $\times$  NA 1.42 oil objective (Olympus). The different fluorophores were excited at 405 nm (Hoechst), 488 nm (EGFP), and 559 nm (MitoTracker), and Kalman averaging ( $n = 3$ , sequential) was used to record multichannel images. The fluorescent signals emitted from EGFP, MitoTracker, and Hoechst were acquired through green, red, and blue channels, respectively, and merged.

### Preparation of mitoplast extracts enriched for inner mitochondrial membrane proteins

Human cells were grown in  $\varnothing$ 15-cm plates until 50–80% confluent, washed once with PBS, and harvested by scraping in 2 ml of PBS. Cells were centrifuged (3 min, 550  $\times g$ ), PBS removed, and cell pellets were frozen at  $-20^{\circ}\text{C}$ , until needed. Preparation of cell extracts enriched for inner mitochondrial membrane proteins was performed at  $4^{\circ}\text{C}$ , based on a protocol described previously (43), with modifications (21). Protein concentration in extracts was determined using Pierce BCA Protein Assay Kit (Thermo Fisher Scientific).

Frozen fragments of rat organs or pellets of *C. elegans* were thawed on ice, resuspended in PBS containing 2 mg/ml digitonin and protease inhibitor mix (Sigma-Aldrich, P8340), and mechanically fragmented by vortexing with sharp glass beads. Nonsolubilized material and glass beads were removed by centrifugation (500  $\times g$ , 2 min). The supernatant was then used to prepare mitoplast extracts, similarly as described above.

### Western blot analysis

Proteins present in mitoplast extracts (30  $\mu$ g), prepared as described above, were resolved by SDS-PAGE and transferred to PVDF Immobilon-FL transfer membrane (Merck), which was stained with Ponceau S and blocked using Odyssey<sup>®</sup> Blocking Buffer (TBS) (Li-Cor) diluted 1:1 (v/v) in TBS. The membrane was then incubated with primary antibodies: mouse anti-FLAG (F1804, Sigma-Aldrich), mouse anti-ANT2 (H00000292-B01P, Abnova), mouse anti-ATP5A (ab14748, Abcam), rabbit anti-ATPSc (ab181243, Abcam), rabbit anti-COX IV (ab16056, Abcam), rabbit anti-methylated lysine (ab23366, Abcam), or rabbit anti-trimethylated lysine (ab76118, Abcam) diluted in Odyssey<sup>®</sup> Blocking Buffer mixed 1:1 (v/v) with TBS, containing 0.05% Tween 20. The primary

antibodies were detected with Li-Cor secondary antibodies coupled with IR fluorescent dyes, either goat anti-mouse IRDye<sup>®</sup> 680RD or goat anti-rabbit IRDye<sup>®</sup> 800CW, according to the manufacturer's instructions, and visualized using Li-Cor Odyssey CLx Imaging System. When needed, the same membrane was reprobed with different primary and secondary antibodies, without stripping. Precision Plus Protein Dual Color Standards (Bio-Rad) or Cameleon Duo Prestained Protein Ladder (Li-Cor) was used to evaluate the size of polypeptides visualized by Western blotting.

### Mass spectrometry analysis

Proteins present in mitoplast extracts were resolved by SDS-PAGE, stained with Coomassie Blue, and the portion of the gel containing the protein of interest was excised and subjected to in-gel chymotrypsin (Roche) digestion. Peptides resulting from proteolytic digestion were analyzed by LC coupled to MS, similarly as described previously (19).

MS data were analyzed using in-house maintained human, rat, and *C. elegans* protein sequence databases using SEQUEST<sup>™</sup> and Proteome Discoverer<sup>™</sup> (Thermo Fisher Scientific). The mass tolerances of a fragment ion and a parent ion were set to 0.5 Da and 10 ppm, respectively. Methionine oxidation, cysteine carbamido-methylation, lysine and arginine methylation were selected as variable modifications. MS/MS spectra of peptides corresponding to methylated ANT and mitochondrial phosphate carrier, were manually searched by Qual Browser (v2.0.7).

### Measurement of mitochondrial respiration by Seahorse

HAP1 cells, or derivatives thereof, were seeded in three T75 flasks ( $8 \times 10^6$  cells/flask) and grown for 48 h at  $37^{\circ}\text{C}$ . Mitochondria were isolated from cells according to a described protocol (44). To measure Complex II-driven respiration, isolated mitochondria (15  $\mu$ g of mitochondrial protein) were added into noncoated XF24 plates, in MAS buffer (220 mM D-mannitol, 70 mM sucrose, 10 mM  $\text{KH}_2\text{PO}_4$ , 5 mM  $\text{MgCl}_2$ , 2 mM HEPES, 1 mM EGTA, and 0.2% (w/v) of fatty acid-free BSA, pH 7.2) supplemented with 10 mM succinate and 2  $\mu$ M rotenone. OCRs were measured under basal conditions, and after sequential addition of ADP (2 mM), oligomycin (3.2  $\mu$ M), FCCP (4  $\mu$ M), and AntA (4  $\mu$ M). Each assay cycle consisted of 1 min of mixing and 3 min of OCR measurements. For each condition, three cycles were used to determine the average OCR under given condition, *i.e.*  $\text{OCR}_{\text{basal}}$ ,  $\text{OCR}_{\text{ADP}}$ ,  $\text{OCR}_{\text{oligomycin}}$ ,  $\text{OCR}_{\text{FCCP}}$ , and  $\text{OCR}_{\text{AntA}}$ . The measured OCRs are expressed in pmol of  $\text{O}_2$  consumed per min (pmol/min). OCRs measured under different conditions were used to calculate the individual states of mitochondrial respiration, *i.e.* State II, basal respiration ( $\text{OCR}_{\text{basal}} - \text{OCR}_{\text{AntA}}$ ); State III, respiration stimulated by ATP synthesis from ADP and phosphate ( $\text{OCR}_{\text{ADP}} - \text{OCR}_{\text{AntA}}$ ); State IV<sub>o</sub>, respiration because of proton leak in the presence of oligomycin ( $\text{OCR}_{\text{oligomycin}} - \text{OCR}_{\text{AntA}}$ ); and State III<sub>u</sub>, respiration in presence of mitochondrial uncoupling agent FCCP ( $\text{OCR}_{\text{FCCP}} - \text{OCR}_{\text{AntA}}$ ). An individual experiment consisted of five replicates of OCR measurements, using mitochondria (15  $\mu$ g of mitochondrial protein) isolated from each of the four HAP1-derived cell lines. The data within an individual experiment were normalized for State II res-

piration measured in mitochondria isolated from WT cells, and combined results from two such individual and independent experiments are reported as % of State II respiration observed in WT.

### Statistical analysis

The independent two-sample Student's *t* test was used to evaluate the probability (*p* value) that the means of two populations are not different.

**Author contributions**—J. M. and P. Ø. F. conceptualization; J. M., H. L. D. M. W., A. Y. Y. H., N. E., and P. Ø. F. resources; J. M., H. L. D. M. W., A. Y. Y. H., and A. M. data curation; J. M., H. L. D. M. W., A. M., N. E., and P. Ø. F. formal analysis; J. M., N. E., and P. Ø. F. supervision; J. M., H. L. D. M. W., R. P., A. Y. Y. H., and A. M. validation; J. M., H. L. D. M. W., R. P., A. Y. Y. H., and A. M. investigation; J. M. and P. Ø. F. visualization; J. M., H. L. D. M. W., R. P., A. M., N. E., and P. Ø. F. methodology; J. M. and P. Ø. F. writing—original draft; J. M., H. L. D. M. W., R. P., N. E., and P. Ø. F. writing—review and editing; P. Ø. F. funding acquisition; P. Ø. F. project administration.

**Acknowledgments**—We thank Dr. Magnus Jakobsson for assistance during the initial phase of this project. We thank Ingrid F. Kjønstad for technical assistance with cloning. We thank Dr. Marianne Fyhn from Department of Biosciences, University of Oslo, for providing us with rat organs. We thank Dr. Hilde Nilsen from Oslo University Hospital for providing us with *Caenorhabditis elegans*. We thank Dr. Boudewijn Burgering from University Medical Center Utrecht for the use of Seahorse analyzer instrument. We thank Oslo NorMIC Imaging Platform (Department of Biosciences, University of Oslo) for the use of cell imaging equipment.

### References

- Schubert, H. L., Blumenthal, R. M., and Cheng, X. (2003) Many paths to methyltransferase: A chronicle of convergence. *Trends Biochem. Sci.* **28**, 329–335 [CrossRef Medline](#)
- Petrossian, T. C., and Clarke, S. G. (2011) Uncovering the human methyltransferasome. *Mol. Cell Proteomics* **10**, M110.000976 [CrossRef Medline](#)
- Schubert, H. L., Blumenthal, R. M., and Cheng, X. (2006) 1 Protein methyltransferases: Their distribution among the five structural classes of AdoMet-dependent methyltransferases. *Enzymes* **24**, 3–28 [CrossRef Medline](#)
- Bedford, M. T. (2007) Arginine methylation at a glance. *J. Cell Sci.* **120**, 4243–4246 [CrossRef Medline](#)
- Figaro, S., Scrima, N., Buckingham, R. H., and Heurgué-Hamard, V. (2008) HemK2 protein, encoded on human chromosome 21, methylates translation termination factor eRF1. *FEBS Lett.* **582**, 2352–2356 [CrossRef Medline](#)
- Moore, K. E., and Gozani, O. (2014) An unexpected journey: Lysine methylation across the proteome. *Biochim. Biophys. Acta* **1839**, 1395–1403 [CrossRef Medline](#)
- Webb, K. J., Zurita-Lopez, C. I., Al-Hadid, Q., Laganowsky, A., Young, B. D., Lipson, R. S., Souda, P., Faull, K. F., Whitelegge, J. P., and Clarke, S. G. (2010) A novel 3-methylhistidine modification of yeast ribosomal protein Rpl3 is dependent upon the YIL110W methyltransferase. *J. Biol. Chem.* **285**, 37598–37606 [CrossRef Medline](#)
- Falnes, P. Ø., Jakobsson, M. E., Davydova, E., Ho, A. Y., and Małecki, J. (2016) Protein lysine methylation by seven-β-strand methyltransferases. *Biochem. J.* **473**, 1995–2009 [CrossRef Medline](#)
- Cloutier, P., Lavallee-Adam, M., Faubert, D., Blanchette, M., and Coulombe, B. (2013) A newly uncovered group of distantly related lysine methyltransferases preferentially interact with molecular chaperones to regulate their activity *PLoS Genet.* **9**, e1003210 [CrossRef Medline](#)
- Feng, Q., Wang, H., Ng, H. H., Erdjument-Bromage, H., Tempst, P., Struhl, K., and Zhang, Y. (2002) Methylation of H3-lysine 79 is mediated by a new family of HMTases without a SET domain. *Curr. Biol.* **12**, 1052–1058 [CrossRef Medline](#)
- Hamey, J. J., Winter, D. L., Yagoub, D., Overall, C. M., Hart-Smith, G., and Wilkins, M. R. (2016) Novel N-terminal and lysine methyltransferases that target translation elongation factor 1A in yeast and human. *Mol. Cell. Proteomics* **15**, 164–176 [CrossRef Medline](#)
- Hamey, J. J., Wienert, B., Quinlan, K. G. R., and Wilkins, M. R. (2017) METTL21B is a novel human lysine methyltransferase of translation elongation factor 1A: Discovery by CRISPR/Cas9 knockout. *Mol. Cell. Proteomics* **16**, 2229–2242 [CrossRef Medline](#)
- Jakobsson, M. E., Moen, A., Bousset, L., Egge-Jacobsen, W., Kernstock, S., Melki, R., and Falnes, P. Ø. (2013) Identification and characterization of a novel human methyltransferase modulating Hsp70 function through lysine methylation. *J. Biol. Chem.* **288**, 27752–27763 [CrossRef Medline](#)
- Jakobsson, M. E., Małecki, J., Nilges, B. S., Moen, A., Leidel, S. A., and Falnes, P. Ø. (2017) Methylation of human eukaryotic elongation factor alpha (eEF1A) by a member of a novel protein lysine methyltransferase family modulates mRNA translation. *Nucleic Acids Res.* **45**, 8239–8254 [CrossRef Medline](#)
- Jakobsson, M. E., Małecki, J. M., Halabelian, L., Nilges, B. S., Pinto, R., Kudithipudi, S., Munk, S., Davydova, E., Zuhairi, F. R., Arrowsmith, C. H., Jeltsch, A., Leidel, S. A., Olsen, J. V., and Falnes, P. Ø. (2018) The dual methyltransferase METTL13 targets N terminus and Lys55 of eEF1A and modulates codon-specific translation rates. *Nat. Commun.* **9**, 3411 [CrossRef Medline](#)
- Kernstock, S., Davydova, E., Jakobsson, M., Moen, A., Pettersen, S., Mælandsmo, G. M., Egge-Jacobsen, W., and Falnes, P. Ø. (2012) Lysine methylation of VCP by a member of a novel human protein methyltransferase family. *Nat. Commun.* **3**, 1038 [CrossRef Medline](#)
- Liu, S., Hausmann, S., Carlson, S. M., Fuentes, M. E., Francis, J. W., Pillai, R., Lofgren, S. M., Hulea, L., Tandoc, K., Lu, J., Li, A., Nguyen, N. D., Caporicci, M., Kim, M. P., Maitra, A., et al. (2019) METTL13 methylation of eEF1A increases translational output to promote tumorigenesis. *Cell* **176**, 491–504.e21 [CrossRef Medline](#)
- Małecki, J., Ho, A. Y., Moen, A., Dahl, H. A., and Falnes, P. Ø. (2015) Human METTL20 is a mitochondrial lysine methyltransferase that targets the β subunit of electron transfer flavoprotein (ETFβ) and modulates its activity. *J. Biol. Chem.* **290**, 423–434 [CrossRef Medline](#)
- Małecki, J., Aileni, V. K., Ho, A. Y. Y., Schwarz, J., Moen, A., Sørensen, V., Nilges, B. S., Jakobsson, M. E., Leidel, S. A., and Falnes, P. Ø. (2017) The novel lysine specific methyltransferase METTL21B affects mRNA translation through inducible and dynamic methylation of Lys-165 in human eukaryotic elongation factor 1 alpha (eEF1A). *Nucleic Acids Res.* **45**, 4370–4389 [CrossRef Medline](#)
- Małecki, J., Jakobsson, M. E., Ho, A. Y. Y., Moen, A., Rustan, A. C., and Falnes, P. Ø. (2017) Uncovering human METTL12 as a mitochondrial methyltransferase that modulates citrate synthase activity through metabolite-sensitive lysine methylation. *J. Biol. Chem.* **292**, 17950–17962 [CrossRef Medline](#)
- Małecki, J. M., Willemsen, H. L. D. M., Pinto, R., Ho, A. Y. Y., Moen, A., Kjønstad, I. F., Burgering, B. M. T., Zwartkruis, F., Eijkelkamp, N., and Falnes, P. Ø. (2019) Lysine methylation by the mitochondrial methyltransferase FAM173B optimizes the function of mitochondrial ATP synthase. *J. Biol. Chem.* **294**, 1128–1141 [CrossRef Medline](#)
- Rhein, V. F., Carroll, J., He, J., Ding, S., Fearnley, I. M., and Walker, J. E. (2014) Human METTL20 methylates lysine residues adjacent to the recognition loop of the electron transfer flavoprotein in mitochondria. *J. Biol. Chem.* **289**, 24640–24651 [CrossRef Medline](#)
- Rhein, V. F., Carroll, J., Ding, S., Fearnley, I. M., and Walker, J. E. (2017) Human METTL12 is a mitochondrial methyltransferase that modifies citrate synthase. *FEBS Lett.* **591**, 1641–1652 [CrossRef Medline](#)
- Shimazu, T., Barjau, J., Sohtome, Y., Sodeoka, M., and Shinkai, Y. (2014)

## Methylation of adenine nucleotide translocase by FAM173A

- seven-beta-strand methyltransferase METTL10 to be an EF1A1 lysine methyltransferase. *PLoS One* **9**, e105394 [CrossRef Medline](#)
25. Hornbeck, P. V., Kornhauser, J. M., Tkachev, S., Zhang, B., Skrzypek, E., Murray, B., Latham, V., and Sullivan, M. (2012) PhosphoSitePlus: A comprehensive resource for investigating the structure and function of experimentally determined post-translational modifications in man and mouse. *Nucleic Acids Res.* **40**, D261–D270 [CrossRef Medline](#)
  26. Chen, R., Fearnley, I. M., Palmer, D. N., and Walker, J. E. (2004) Lysine 43 is trimethylated in subunit C from bovine mitochondrial ATP synthase and in storage bodies associated with Batten disease. *J. Biol. Chem.* **279**, 21883–21887 [CrossRef Medline](#)
  27. Walpole, T. B., Palmer, D. N., Jiang, H., Ding, S., Fearnley, I. M., and Walker, J. E. (2015) Conservation of complete trimethylation of lysine-43 in the rotor ring of c-subunits of metazoan adenosine triphosphate (ATP) synthases. *Mol. Cell Proteomics* **14**, 828–840 [CrossRef Medline](#)
  28. Klingenberg, M., Riccio, P., and Aquila, H. (1978) Isolation of the ADP, ATP carrier as the carboxyatractylate · protein complex from mitochondria. *Biochim. Biophys. Acta* **503**, 193–210 [CrossRef Medline](#)
  29. Brenner, C., Subramaniam, K., Pertuiset, C., and Pervaiz, S. (2011) Adenine nucleotide translocase family: Four isoforms for apoptosis modulation in cancer. *Oncogene* **30**, 883–895 [CrossRef Medline](#)
  30. Klingenberg, M. (2008) The ADP and ATP transport in mitochondria and its carrier. *Biochim. Biophys. Acta* **1778**, 1978–2021 [CrossRef Medline](#)
  31. Stepien, G., Torrioni, A., Chung, A. B., Hodge, J. A., and Wallace, D. C. (1992) Differential expression of adenine nucleotide translocator isoforms in mammalian tissues and during muscle cell differentiation. *J. Biol. Chem.* **267**, 14592–14597 [Medline](#)
  32. Aquila, H., Misra, D., Eulitz, M., and Klingenberg, M. (1982) Complete amino acid sequence of the ADP/ATP carrier from beef heart mitochondria. *Hoppe-Seyler's Z. Physiol. Chem.* **363**, 345–349 [CrossRef Medline](#)
  33. Guo, A., Gu, H., Zhou, J., Mulhern, D., Wang, Y., Lee, K. A., Yang, V., Aguiar, M., Kornhauser, J., Jia, X., Ren, J., Beausoleil, S. A., Silva, J. C., Vemulapalli, V., Bedford, M. T., and Comb, M. J. (2014) Immunoaffinity enrichment and mass spectrometry analysis of protein methylation. *Mol. Cell Proteomics* **13**, 372–387 [CrossRef Medline](#)
  34. Pebay-Peyroula, E., Dahout-Gonzalez, C., Kahn, R., Trézéguet, V., Lauquin, G. J., and Brandolin, G. (2003) Structure of mitochondrial ADP/ATP carrier in complex with carboxyatractyloside. *Nature* **426**, 39–44 [CrossRef Medline](#)
  35. Duncan, A. L., Robinson, A. J., and Walker, J. E. (2016) Cardiolipin binds selectively but transiently to conserved lysine residues in the rotor of metazoan ATP synthases. *Proc. Natl. Acad. Sci. U.S.A.* **113**, 8687–8692 [CrossRef Medline](#)
  36. Nury, H., Dahout-Gonzalez, C., Trézéguet, V., Lauquin, G., Brandolin, G., and Pebay-Peyroula, E. (2005) Structural basis for lipid-mediated interactions between mitochondrial ADP/ATP carrier monomers. *FEBS Lett.* **579**, 6031–6036 [CrossRef Medline](#)
  37. Hedger, G., Rouse, S. L., Domański, J., Chavent, M., Koldsø, H., and Sansom, M. S. (2016) Lipid-loving ANTs: Molecular simulations of cardiolipin interactions and the organization of the adenine nucleotide translocase in model mitochondrial membranes. *Biochemistry* **55**, 6238–6249 [CrossRef Medline](#)
  38. Claypool, S. M., Oktay, Y., Boonthueung, P., Loo, J. A., and Koehler, C. M. (2008) Cardiolipin defines the interactome of the major ADP/ATP carrier protein of the mitochondrial inner membrane. *J. Cell Biol.* **182**, 937–950 [CrossRef Medline](#)
  39. Ito, S., Tan, L. J., Andoh, D., Narita, T., Seki, M., Hirano, Y., Narita, K., Kuraoka, I., Hiraoka, Y., and Tanaka, K. (2010) MMXD, a TFIIF-independent XPD-MMS19 protein complex involved in chromosome segregation. *Mol. Cell* **39**, 632–640 [CrossRef Medline](#)
  40. Lu, Y. W., Acoba, M. G., Selvaraju, K., Huang, T. C., Nirujogi, R. S., Sathe, G., Pandey, A., and Claypool, S. M. (2017) Human adenine nucleotide translocases physically and functionally interact with respirasomes. *Mol. Biol. Cell* **28**, 1489–1506 [CrossRef Medline](#)
  41. Davydova, E., Ho, A. Y., Malecki, J., Moen, A., Enserink, J. M., Jakobsson, M. E., Loenarz, C., and Falnes, P. Ø. (2014) Identification and characterization of a novel evolutionarily conserved lysine-specific methyltransferase targeting eukaryotic translation elongation factor 2 (eEF2). *J. Biol. Chem.* **289**, 30499–30510 [CrossRef Medline](#)
  42. Waterhouse, A. M., Procter, J. B., Martin, D. M., Clamp, M., and Barton, G. J. (2009) Jalview Version 2—a multiple sequence alignment editor and analysis workbench. *Bioinformatics* **25**, 1189–1191 [CrossRef Medline](#)
  43. Klement, P., Nijtmans, L. G., Vandenbogert, C., and Houstek, J. (1995) Analysis of oxidative phosphorylation complexes in cultured human fibroblasts and amniocytes by blue-native-electrophoresis using mitoplasts isolated with the help of digitonin. *Anal. Biochem.* **231**, 218–224 [CrossRef Medline](#)
  44. Iuso, A., Repp, B., Biagosch, C., Terrile, C., and Prokisch, H. (2017) Assessing mitochondrial bioenergetics in isolated mitochondria from various mouse tissues using Seahorse XF96 analyzer. *Methods Mol. Biol.* **1567**, 217–230 [CrossRef Medline](#)
  45. Watt, I. N., Montgomery, M. G., Runswick, M. J., Leslie, A. G., and Walker, J. E. (2010) Bioenergetic cost of making an adenosine triphosphate molecule in animal mitochondria. *Proc. Natl. Acad. Sci. U.S.A.* **107**, 16823–16827 [CrossRef Medline](#)

**Human FAM173A is a mitochondrial lysine-specific methyltransferase that targets adenine nucleotide translocase and affects mitochondrial respiration**

Jedrzej M. Malecki, Hanneke L. D. M. Willemsen, Rita Pinto, Angela Y. Y. Ho, Anders Moen, Niels Eijkelkamp and Pål Ø. Falnes

*J. Biol. Chem.* 2019, 294:11654-11664.

doi: 10.1074/jbc.RA119.009045 originally published online June 18, 2019

---

Access the most updated version of this article at doi: [10.1074/jbc.RA119.009045](https://doi.org/10.1074/jbc.RA119.009045)

Alerts:

- [When this article is cited](#)
- [When a correction for this article is posted](#)

[Click here](#) to choose from all of JBC's e-mail alerts

This article cites 45 references, 20 of which can be accessed free at <http://www.jbc.org/content/294/31/11654.full.html#ref-list-1>